Journal of Maps

ISSN: (Print) 1744-5647 (Online) Journal homepage: http://www.tandfonline.com/loi/tjom20

Tectonics, ore bodies, and gamma-ray logging of the Variscan basement, southern Gennargentu massif (central Sardinia, Italy)

Mattia Alessio Meloni, Giacomo Oggiano, Antonio Funedda, Marco Pistis & Ulf Linnemann

To cite this article: Mattia Alessio Meloni, Giacomo Oggiano, Antonio Funedda, Marco Pistis & Ulf Linnemann (2017) Tectonics, ore bodies, and gamma-ray logging of the Variscan basement, southern Gennargentu massif (central Sardinia, Italy), Journal of Maps, 13:2, 196-206, DOI: 10.1080/17445647.2017.1287601

To link to this article: http://dx.doi.org/10.1080/17445647.2017.1287601

JOURNAL OF MAPS, 2017
VOL. 13, NO. 02, 196–206
http://dx.doi.org/10.1080/17445647.2017.1287601

Taylor & Francis
Taylor & Francis Group

SCIENCE

OPEN ACCESS

Tectonics, ore bodies, and gamma-ray logging of the Variscan basement, southern Gennargentu massif (central Sardinia, Italy)

Mattia Alessio Meloni[a], Giacomo Oggiano [a], Antonio Funedda[b], Marco Pistis[b] and Ulf Linnemann[c]

[a]Dipartimento di Scienze della natura e del territorio (DIPNET), Università degli studi di Sassari, Sassari, Italy; [b]Dipartimento di Scienze chimiche e geologiche, Università degli studi di Cagliari, Cagliari, Italy; [c]Senckenberg Naturhistorische Sammlungen Dresden, Museum für Mineralogie und Geologie, Sektion Geochronologie, GeoPlasma Lab Dresden, Germany

ABSTRACT

We present a structural geological map (1:14,000 scale) that covers a 100 km^2 area of Variscan basement rocks exposed in central Sardinia. The mapped area is located between 39°56′20″ N 9°04′59″ E (northwestern corner) and 39°51′47″ N 9°13′16″ E (southeastern corner) on the southern slope of the Gennargentu massif, surrounding the mining village of Gadoni. This village was the hub of a mining district in central Sardinia. The region extends between the external and inner nappe zones of the Variscan orogenic wedge of Sardinia. Despite significant mining, the area lacked an up-to-date structural and stratigraphic synthesis comparable to that achieved in the southern Sardinia. This gap in knowledge was due to: (i) more complex structural deformation; (ii) slightly higher grade regional metamorphism including a late Variscan high-temperature overprint; (iii) difficulty in distinguishing terrigenous stratigraphic units that belong to different tectonic units; and (iv) the absence of key stratigraphic marker for resolve complex structures in the uppermost tectonic unit. Integration of field mapping, structural analysis, portable gamma-ray spectroscopy, and zircon U-Pb ages of intrusive rocks has enabled a new geological map and cross-sections. These contributions synthesize the collisional and postcollisional evolution of the region and its relationship with ore genesis.

ARTICLE HISTORY
Received 23 August 2016
Revised 29 December 2016
Accepted 24 January 2017

KEYWORDS
Variscan chain; structural map; gamma-ray spectroscopy; skarn; Sardinia

1. Introduction

The nappe zone of the Sardinian Variscan chain consists of a stack of tectonic units affected by low-grade metamorphism, which are classically subdivided into external and internal nappes (Figure 1). The external nappes have a low- to very low-grade metamorphic overprint and share a well-defined stratigraphy, constrained by paleontology, with few variations between different tectonic units. Due to slightly higher grade regional metamorphism and more intense deformation, the internal nappes have a poorly defined stratigraphy, which has limited the interpretation of their structural framework. Moreover, these units lack the distinctive lithological marker horizon of Middle Ordovician calk-alkaline meta-volcanic rocks, which overlie the Sardic Unconformity and characterize the external nappes (Gaggero, Oggiano, Funedda, & Buzzi, 2012; Oggiano, Gaggero, Funedda, Buzzi, & Tiepolo, 2010).

The study area is located in central Sardinia (refer to Main Map and Figure 2), where the main tectonic unit of the internal nappe (i.e. the Barbagia Unit, previously known as the 'Postgotlandiano'; Minzoni, 1988; Vai & Cocozza, 1974) overrides the Meana Sardo Unit, which occupies the structurally highest position in the stack of external nappes (Carmignani, Oggiano, Funedda, Conti, & Pasci, 2015; Funedda, Meloni, & Loi, 2015). The Barbagia Unit (Pertusati et al., 2002) mainly consists of a continuous meta-sedimentary sequence of pelite to arenite, where no fossils remnants are preserved. The Meana Sardo Unit is well exposed in some tectonic windows, where Ordovician clastic sediments and volcanic rocks, Silurian black shale, and Silurian–Devonian limestone affected by low-grade metamorphism are clearly revealed. However, the terrigenous portion of the Meana Sardo Unit is barely distinguishable from the terrigenous sequences of the Barbagia Unit. Extensive skarn containing magnetite, base metals, sulfides, and calc-silicates (Dessau, 1937) characterize the study area, presenting additional difficulties for interpreting the stratigraphy and structural framework.

To overcome these challenges, detailed geological mapping was performed with the aid of a portable gamma-ray spectrometer to help distinguish lithotectonic units on the basis of sedimentary provenance and facies (Šimíček, Bàbek, & Leichmann, 2012). These analyses were integrated zircon U–Pb

CONTACT Mattia Alessio Meloni giacoggi@uniss.it Dipartimento di Scienze della natura e del territorio (DIPNET), Università degli studi di Sassari, Via Muroni 25, 07100 Sassari, Italy

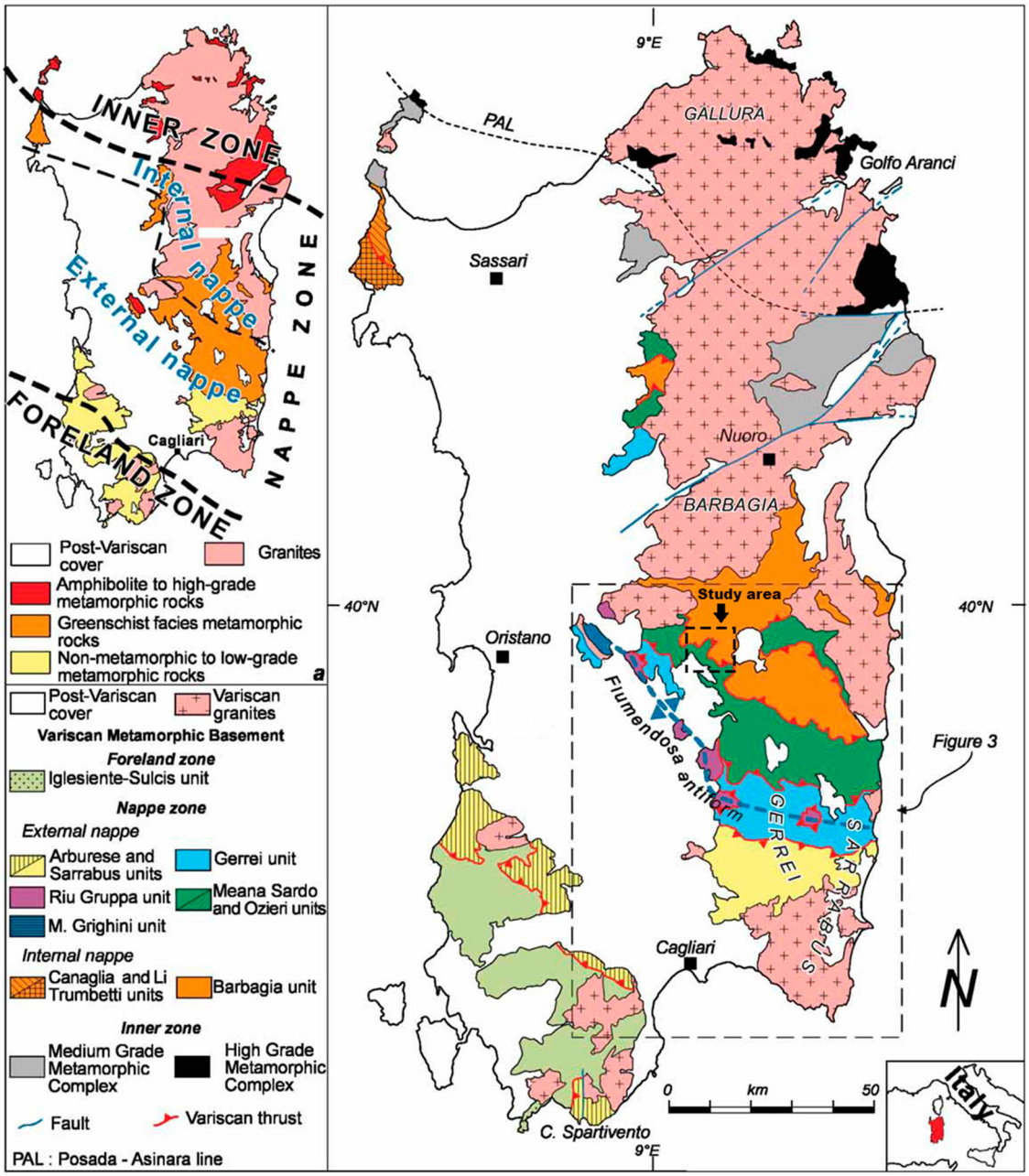

Figure 1. Tectono-metamorphic sketch map of the Variscan basement in Sardinia (after Funedda et al., 2015).

geochronology performed on late-stage Variscan intrusions. Thus, this study contributes to the elucidation of relationships between different tectonic units and the role of collisional and post-collisional tectonics in ore genesis in the Sardinian Variscan chain.

2. Methods

Geological mapping was performed at 1:10,000 scale to highlight the spatial relationships between geological units. The first several drafts of the map were hand-drawn and only the final version of the map, legend, cross-sections, and sketches were constructed electronically using dedicated software.

Geological cross-sections were made to provide a 3D geological model of the study area. Along northeast-striking cross-sections (A–A1, B–B1, and D–D1) the data were projected parallel to the LD_1 (Flumendosa phase) axis, which trends approximately 20° toward 130°. Therefore, structures cropping out on the northwestern side of the cross-section traces are projected underground. Along the west–northwest-striking C–C1 cross-section, the data were projected parallel to 20° toward 230° to highlight LD_{1a} structures.

Approximately 100 samples were collected for petrographic analysis, structural analysis, and microanalysis in thin section. Additionally, one sample (GR110) was collected for zircon U–Pb dating. For this technique, mineral separation was carried out using conventional methods, and crystals without fractures, visible inclusions, or compositional zonation were identified by cathodoluminescence analysis with a

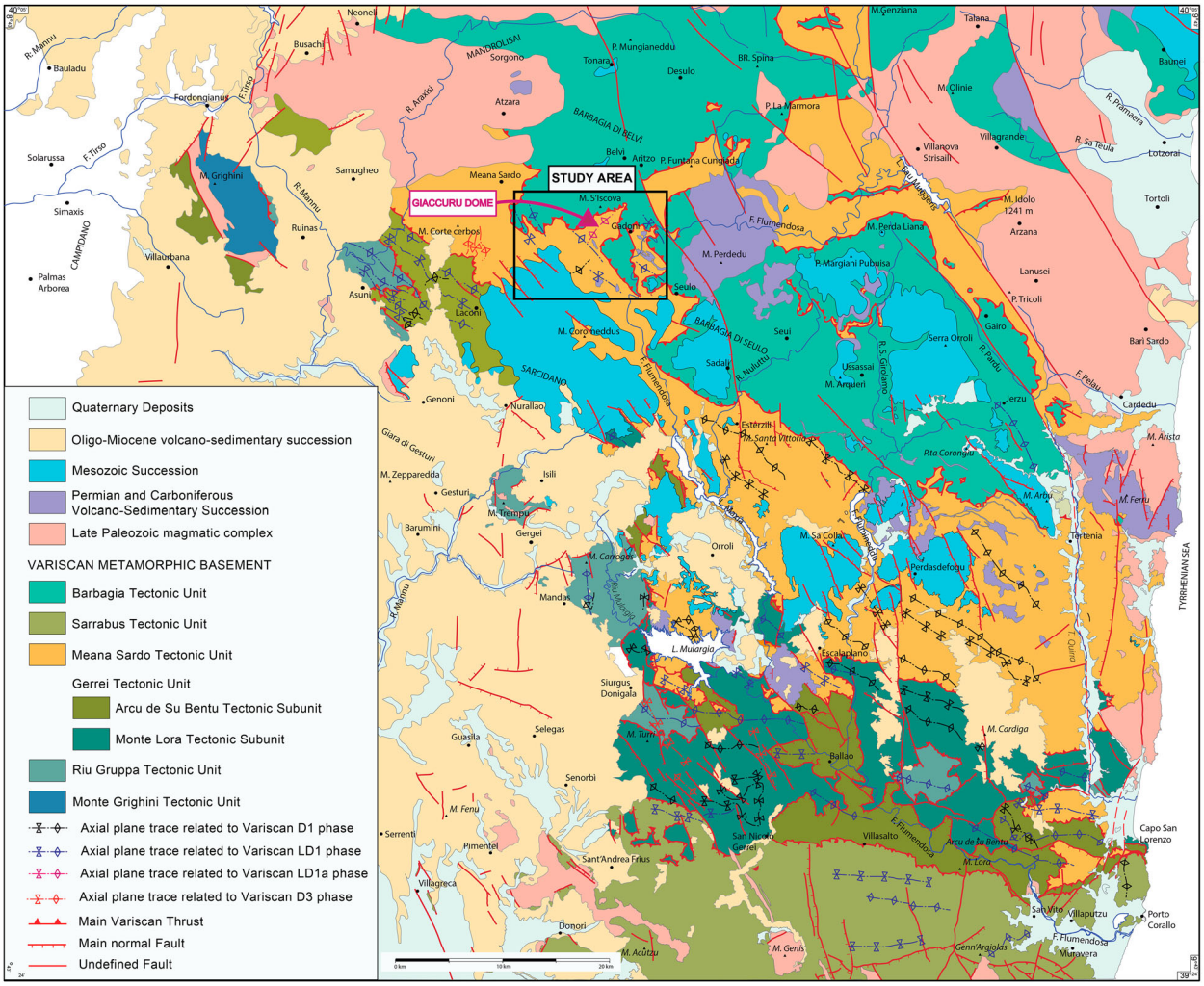

Figure 2. Schematic structural map of the Variscan basement of SE Sardinia (after Funedda et al., 2015).

scanning electron microscope (SEM; JEOL JXA840). Suitable zircon grains were hand-picked and mounted in epoxy resin. Isotopic compositions (^{206}Pb, ^{207}Pb, ^{208}Pb, ^{232}Th, and ^{238}U) were determined using a Thermo-Scientific Element 2 XR sector field inductively coupled plasma mass spectrometer coupled to a New Wave UP-193 Excimer Laser System at the Museum of Mineralogy and Geology, Geochronology Section in Dresden, Germany.

Gamma-ray measurements provided valuable information that substitute for stratigraphic and lithologic markers, which are obscure in this area. Most of the measurements were obtained using an RS-230 Super Spec portable spectrometer and a prototypal spectrometer, which include an NaI(Tl) crystal with a volume of 1 L that is optically coupled to a photomultiplier tube. The system was mounted in a backpack and managed using a notebook computer fitted with a GPS antenna.

Major element oxide compositions were determined by instrumental neutron activation analysis and inductively coupled plasma mass spectrometry at ActLabs (Canada). SEM and electron dispersive spectroscopy analyses were performed on ores at Sassari University in Italy.

3. Lithostratigraphy

In general, the tectonic units of the external nappe zone are lithostratigraphically similar and include Middle Cambrian to early Carboniferous successions. However, there are lithostratigraphic differences between the Meana Sardo Unit, which is an external nappe, and the overriding Barbagia Unit, an internal nappe (Figure 3).

3.1. Meana Sardo Unit (external nappe)

The study area is composed of the formations detailed below, which are described from stratigraphically lowest to highest. For each formation, the corresponding acronym used in the Main Map is provided in parentheses after the formation name.

3.1.1. Arenarie di San Vito (SVI) Formation (Calvino, 1959)

This is the lowermost formation of the Meana Sardo Unit. It is composed of alternating beds of fine- to coarse-grained meta-sandstone, gray–green meta-siltstone, and meta-argillite, with thicknesses varying from cm- to m-scale. The sedimentary structures are

Formation	Average Values			Isotopic Ratios		
	K[%]	U[ppm]	Th[ppm]	U/Th	Th/k	U/K
DOR	0.2	1.75	1.4	1.25	7.00	8.75
GNS	0.5	1	7.7	0.13	15.40	2.00
fp	5.08	6.05	23.43	0.26	4.62	1.19
Gra	4.94	3.84	22.00	0.17	4.45	0.78
Ark	1.75	2.45	11.90	0.21	6.80	1.40
GNN	2.94	2.93	14.14	0.21	4.81	1.00
SGAa	0.84	2.66	7.05	0.38	8.42	3.18
SGA	2.23	14.11	18.14	0.78	8.14	6.33
ORR	3.9	8.78	109.92	0.08	28.18	2.25
ORRa	2.84	3.30	26.06	0.13	9.17	1.16
MSVa	4.93	4.40	18.47	0.24	3.75	0.89
MSVb	2.01	2.82	10.53	0.27	5.24	1.40
MSVc	3.87	3.53	15.21	0.23	3.93	0.91
SVI	2.52	4.00	13.13	0.30	5.21	1.59

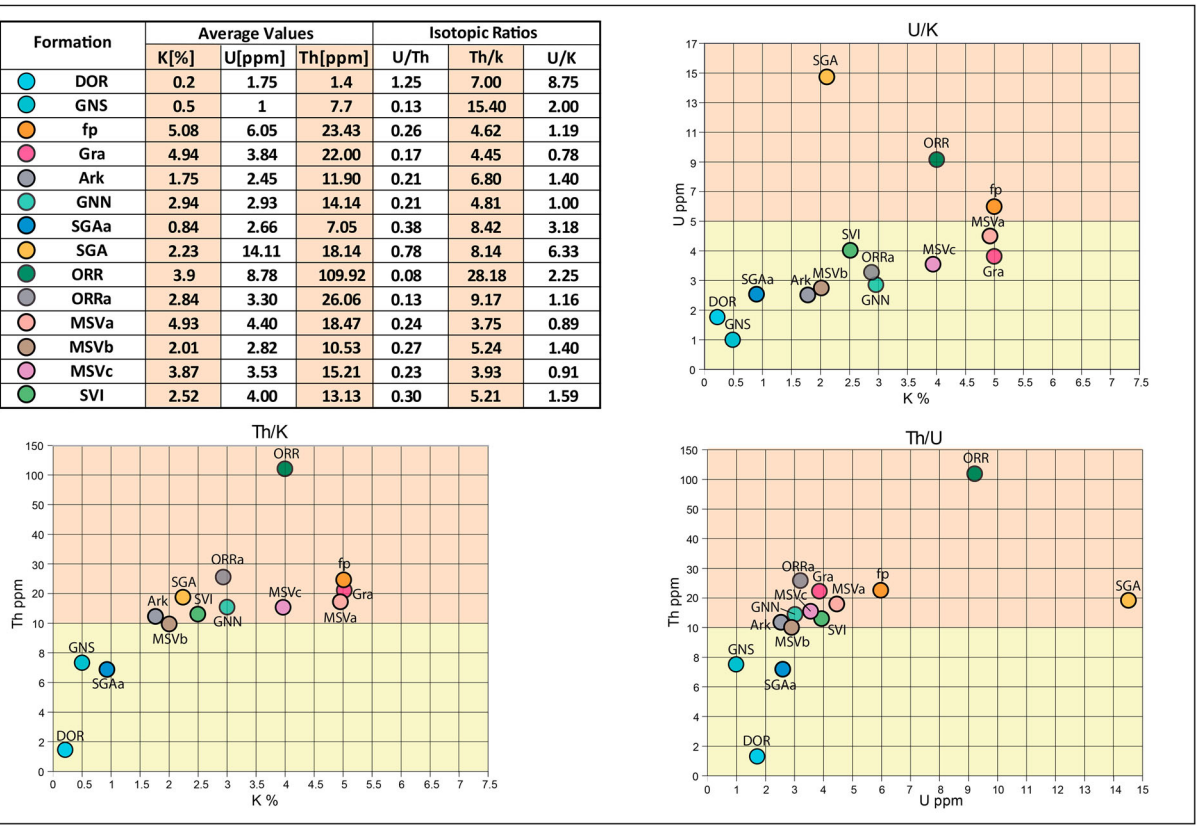

Figure 3. Stratigraphic logs of the Barbagia and Meana Sardo units in the study area and related spectrometric features. Formation acronyms as reported in the Main Map.

generally transposed in hinges of isoclinal folds. Primary bedding is sometimes recognizable in fold limbs, where cross-laminations and ripple structures are preserved. The composition of the sandy fraction is arkose or quartzite. A Middle Cambrian–Early Ordovician age has been obtained from acritarch associations (Di Milia, 1991; Tongiorgi, Albani, & Di Mila, 1984).

3.1.2. Monte Santa Vittoria (MSV) Formation

This formation includes three lithostratigraphic units that were previously informally defined by Minzoni (1975), including the Manixeddu, Monte Corte Cerbos, and Serra Tonnai formations. These lithostratigraphic units are now considered to represent three lithofacies of a single formation of meta-volcanic and meta-epiclastic rocks, which enables streamlined correlations between different external nappes, according to recommendations of the 'Geological Survey of Italy' (Carmignani et al., 2001). All three lithofacies are well represented in the study area. The Manixeddu lithofacies (MSVa) is conglomeratic, and contains clasts of rhyolite and lesser quartzite and older metamorphic rocks. The Monte Corte Cerbos (MSVc) lithofacies is a light gray–green meta-rhyolite, commonly schistose, and contains quartz and feldspar augens. Generally, the top of the formation is composed of green meta-basalt and -andesite (Serra Tonnai lithofacies, MSVb) that contains lepidoblastic chlorite, albite porphyroclasts, and abundant calcite and/or epidote in the groundmass. A Middle–Late Ordovician age has been determined using biostratigraphic and radiometric dating methods (Oggiano et al., 2010).

3.1.3. Orroeledu (ORR) Formation (*Bosellini & Ogniben, 1968*)

This formation records important evidence of the Late Ordovician transgression. It consists of alternating beds of meta-arkose (ORRa), meta-graywacke, and phyllite with a quartz–sericite–chlorite matrix. The fine- to coarse-grained lithic meta-graywacke is often enriched in heavy minerals, which may correspond to shoreface deposits. Titaniferous minerals (rutile, pseudo-rutile, and anatase) are predominant in coarse-grained facies, whereas zircon and monazite are more abundant in fine-grained layers. This formation is comparable in age and depositional environment with meta-sedimentary strata in the Gerrei and Sarrabus units (Figure 2), including the Late Ordovician Rio Canoni Shale (Naud, 1979) and Punta Serpeddì Formation (Loi, Barca, Chauvel, Dabard, & Leone, 1992).

3.1.4. Scisti a Graptoliti (SGA) Formation (*Corradini & Ferretti, 2009*)

This formation is composed of black meta-argillite (originally carbonaceous) alternating with layers of gray meta-siltstone (SGAa). Meta-limestone and

meta-marlstone occur in the upper portion of the sequence. The sequence ranges from Silurian to Early Devonian in age (Corradini, Ferretti, & Serpagli, 1998), and it is an excellent stratigraphic marker within the Meana Sardo Unit.

3.2. Barbagia Unit (internal nappe)

3.2.1. Filladi grigie del Gennargentu (GNN) Formation

In the Gadoni area, this formation is the sole representative of the Barbagia nappe (also known as 'Postgotlandiano'; Vai & Cocozza, 1974) and consists almost exclusively of gray phyllite. It is composed of phyllite, micaceous meta-sandstone and quartzite, which have been affected by greenschist-facies metamorphism. The succession has an apparent thickness of approximately 1000–1500 m. Phyllite is typically silver to light gray in color, with intercalations of dark green material similar to that occurring in the SVI and ORR formations of the Meana Sardo Unit. Locally, quartzite and meta-arkose form horizons with meter-scale thicknesses. In thin section, phyllite is dominated by lepidoblastic muscovite and, to a lesser extent, by other colored phyllosilicates such as stilpnomelane and, possibly, vermiculite. Small albite porphyroblasts are common, as are several prismatic accessory minerals, including tourmaline, monazite, and rutile. This formation is considered to be Cambrian–Ordovician in age (Pertusati et al., 2002).

In some locations, 10 m-thick intervals of quartzite and arkose crop out, and they contain sub-angular to well-rounded quartz grains with a bimodal size distribution that suggests a deposition in littoral environment.

3.3. Late Variscan magmatism

In Sardinia, the intrusions that constitute the Corsica–Sardinia Batholith were emplaced from 285 to 320 Ma. Two main magmatic episodes have been distinguished (Casini, Cuccuru, Maino, & Oggiano, 2015), which occurred at approximately 307 (U2 intrusions) and 290 Ma (U3 intrusions). The earlier magmatic episode generated mainly monzogranite and subordinate granodiorite, whereas the younger magmatic episode mostly produced leucogranite and lesser mafic bodies.

3.3.1. Granodiorite (Gra)

Granodiorite intrusions are exclusively fine-grained and contain several mafic enclaves. They form intrusive bodies that crop out over areas of hundreds of square meters and are hundreds of meters across. These intrusions may represent the counterpart of the Seui volcanic/sub-volcanic complex (Cassinis, Durand, & Ronchi, 2003), located a few kilometers toward the east. In areas where small Granodiorite bodies crop out, the country rocks are affected by an extensive contact aureole, suggesting that they represent the surface expression of a larger intrusion. A fine-grained Granodiorite with mafic enclaves (GR110 sample) yielded a zircon U–Pb age of 299 ± 3 Ma. Hence, the Granodiorite bodies in the Gadoni area are comparable to the U2 intrusions, not really different from other late Variscan plutons in SW Sardinia (e.g. the Arbus Pluton; Cuccuru et al., in press)

3.3.2. Quartz porphyry dikes (Fp)

These hypabyssal rocks are widespread in the study area. The dikes are northwest-trending and exhibit variable petrographic features. Most consist of rhyolite to rhyodacite, and they generally contain phenocrysts of alkali feldspar, quartz, and plagioclase feldspar, as well as aggregates of biotite crystals within a fine-grained groundmass. These dykes may represent feeders to Permian rhyolite lava flows.

3.3.3. Mafic dikes (Mp)

Mafic dikes are smaller and less common than felsic dikes. They are dominantly dioritic and exhibit intersertal texture. They are mainly composed of plagioclase, hornblende, and lesser pyroxene. Biotite, where present, is often altered to chlorite. The mafic dikes are Permian in age.

3.4. Post-Variscan cover rocks

3.4.1. Conglomerate and volcanic breccia (PE)

The Gennargentu Unit is locally unconformably capped by epiclastic deposits that are a few meters thick. They contain metamorphic and volcanic clasts within a fine-grained matrix of devitrified ash. These epiclastic rocks are estimated to have been deposited in the early Permian.

3.4.2. Genna Selole (GNS) Formation

This formation forms the base of the Jurassic cover sequence in the study area. It consists of continental to transitional siliciclastic deposits (Costamagna, Barca, & Lecca, 2007), including quartz conglomerate and gray siltstone that contains lignite seams and clay. Based on palynomorphs, the age is interpreted to be Bajocian–Bathonian (Del Rio, 1985; Dieni, Fischer, Massari, Salard-Cheboldaeff, & Vozenin-Serra, 1983).

3.4.3. Dorgali (DOR) Formation

This formation consists of brown–pink-colored dolostones, which are typically massive and structureless (Amadesi, Cantelli, Carloni, & Rabbi, 1967; Calvino, Dieni, Ferasin, & Piccoli, 1972; Demant & Coulon, 1973; Dieni & Massari, 1985, 1987). Locally, some marl–limestone beds contain abundant brachiopods, echinoids, ammonites, belemnites, and foraminifera

of Middle Jurassic age (Bathonian–Callovian; Dieni & Massari, 1985).

3.4.4. Quaternary deposits (Q)

Quaternary deposits in the study area include Pleistocene and Holocene alluvial and colluvial strata. Fluvial terraces of possible Pleistocene age are only preserved in the Flumendosa valley.

4. Gamma-ray spectroscopy

In the study area, it is typically difficult to distinguish the terrigenous formations of the external nappes (SVI and the ORR Formations) from those of the internal nappes (GNN). In particular, meta-pelitic and meta-arenaceous lithologies lack fossil remnants or other distinct sedimentary features and appear very similar at the outcrop scale. Hence, they are generally impossible to differentiate in the field. Gamma-ray analyses yield additional information (Figure 3) that replaces the need for lithostratigraphic markers and allows the Filladi del Gennargentu Formation to be distinguished from the ORR Formation, and enables the mapping of their tectonic contact. More than 250 gamma-ray measurements, including 200 with the light spectrometer RS-230 Super Spec, were used to investigate the compositions of cm-scale areas. Additional measurements were performed with the prototypal portable spectrometer, which integrates data from areas with 1.5-m radii. During gamma-ray survey some formations produced a unique, clearly recognizable gamma-ray signal, which was very useful for characterizing rock formations according to facies and provenance in agreement with Šimíček et al. (2012).

The ORR Formation and the SGA yielded characteristic gamma-ray signals (Figures 3 and 4). The SGA yielded values of 14.1 for U and 18.1 ppm for Th, with a high U/Th ratio of 0.78, which is typical of a reducing sedimentary environment where primary U was up taken by carbonaceous matter in the form of U4+. One sample of the ORR produced an extremely high maximum total counts per minute (70,226 cpm), with a U content of 8.78 and a Th content of 109.92 ppm. In this location, the U/Th ratio is 0.06 and the average for the ORR is 0.08 which is an order of magnitude lower than that of the SGA. This is because the ORR contains clastic phases that are enriched in U, Th, and possibly rare earth element (REE), such as monazite, zircon, and allanite. The abundance of K (4 wt%) testifies to an originally arkosic composition for the fine-grained clastic component of the ORR. Within the MSV Formation, the MSVc and MSVb produced distinctive gamma-ray signals. In particular, the MSVb (mostly meta-andesite) and MSVc (rhyolitic meta-volcanic rocks) have different K contents of 2 and 5 wt%, respectively.

The Barbagia Unit has relatively uniform values throughout the GNN Formation. The U/Th ratio of 1.0 is similar to that of the GLOSS (global subducting sediment composition; Plank & Langmuir, 1998), as is the Th value of 14 ppm, when plotted on the diagram of Hawkesworth, Turner, McDermott, Peate, and Van Calsteren (1997). The arkosic sections of the formation produced higher values.

5. Structural outline

Variscan tectonism in central Sardinia has been divided into two main events (Dessau, Duchi, Moretti, & Oggiano, 1982). The first event is related to collisional processes and has been subdivided into different syn-metamorphic phases, which are generally referred to as D_1 and D_2 (Carmignani, Cocozza, Ghezzo, Pertusati, & Ricci, 1982; Carosi & Pertusati, 1990; Oggiano, 1994) or, alternatively, as the Gerrei and Meana phases (Conti, Carmignani, & Funedda, 2001). The first two syn-metamorphic phases were responsible for nappe emplacement and the formation of recumbent isoclinal folds with associated axial planar, pervasive, and syn-metamorphic foliation. Late, post-nappe and post-metamorphic shortening has been labeled differently in different parts of the Variscan orogen of Sardinia (Conti et al., 2001), and has been referred to as L_{D1} (Conti & Patta, 1998), the Late Shortening Phase (Gattiglio & Oggiano, 1990), or D_3 (Carosi & Pertusati, 1990). This late shortening gave rise to upright regional folds with wide wave length, which affect the entire nappe zone (Funedda et al., 2015, 2011). Most of these folds that have been identified have north–northwest-trending axes. The second Variscan tectonic event in central Sardinia has been referred to as the Riu Gruppa phase (Conti et al., 2001) or as D3 (Oggiano, 1994), and is linked to the collapse of the Variscan chain. Post-collisional extension occurred throughout the chain, producing different structures according to structural level. In the nappe zone, extensional tectonics occurred within the ductile regime at middle–upper crustal levels, whereas at shallower crustal levels, steep normal faults in the brittle regime generated several Permian–Carboniferous basins. This phase in the nappe zone was widely controlled by the post-nappe collisional structure (Casini & Oggiano, 2008; Conti, Carmignani, Oggiano, Funedda, & Eltrudis, 1999). Along the limbs of principal antiforms, vertical shortening generated: (i) drag folds with centrifugal vergence with respect to the crest line; (ii) inversion of collisional thrusts into low-angle normal shear zones; (iii) exhumation of deeper tectonic units, accompanied by a low-pressure/high-temperature (LP/HT) metamorphic overprint; and (iv) reworking of previously developed foliations.

5.1. Collisional phase (Gerrei and Meana phases)

The collisional phase generated non-cylindrical isoclinal folds, with which the dominant foliation (S_1) is

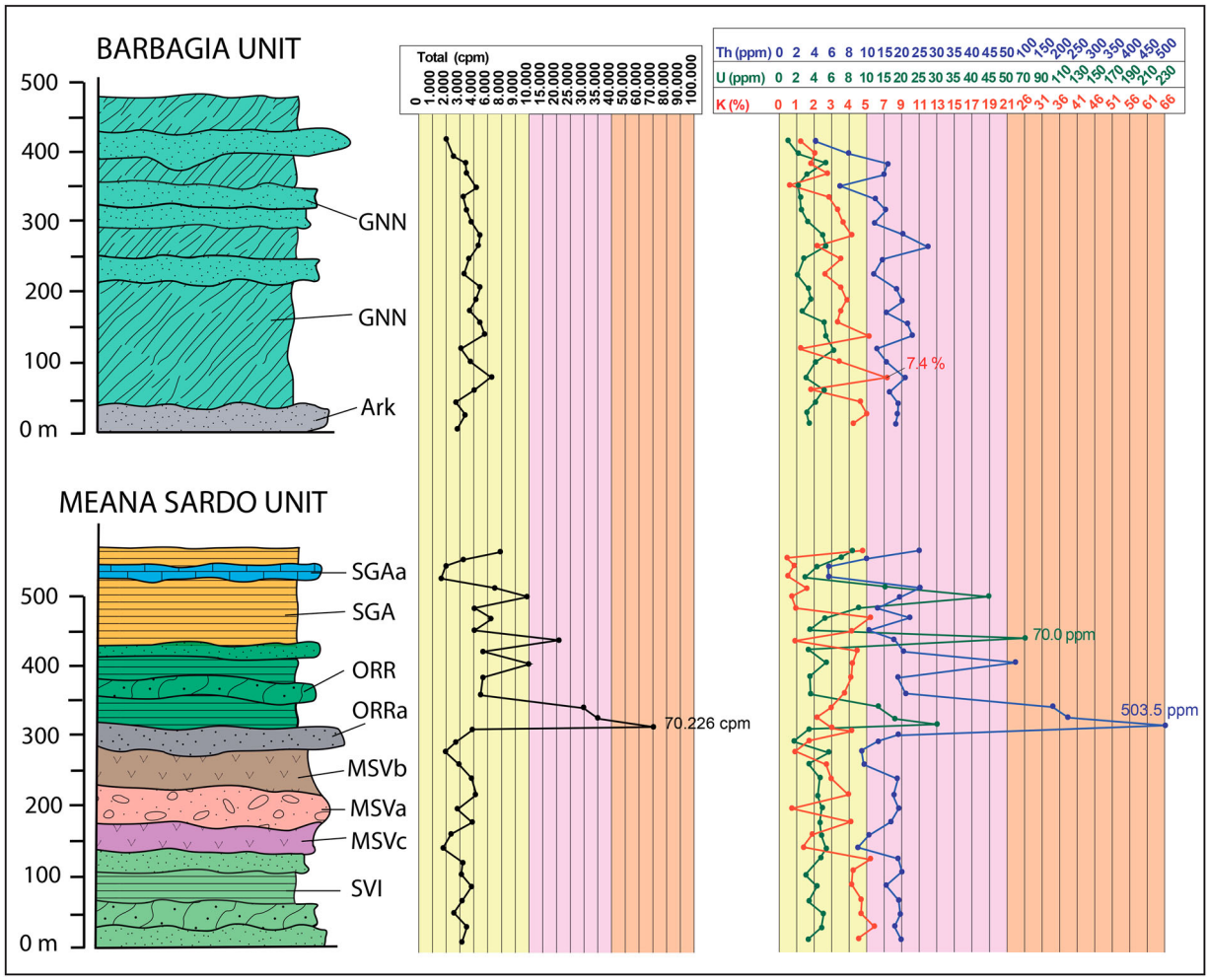

Figure 4. Isotopic characteristics of Paleozoic terrigenous lithologies in the Gadoni area. Formation acronyms as reported in the Main Map.

associated. An older, relict foliation (S_r) is detectable in thin section within micro-lithons defined by S_1, mainly in the Barbagia Unit, but is rarely recognizable in outcrop. The stretching lineation (L_1) associated with S_1 is well-defined, especially by porphyroclasts in meta-volcanic rocks. According to kinematic indicators, including σ- and δ-type asymmetric porphyroclasts and shear bands, the direction of tectonic transport was top-to-the-southwest in the Meana Sardo Unit. In contrast, stretching directions in the Barbagia Unit are more equivocal because structural fabrics exhibit dispersed orientations resulting from more complex post-nappe tectonics (see stereographic projection of Variscan structural elements in the Figure 1 included in the Main Map).

5.2. Post-nappe shortening structures (LD_1 phase)

Mapping in the study area revealed evidence of complex post-nappe shortening, including two nearly orthogonal shortening directions that generated upright folds with axes plunging 10–20° toward 130° (LD_1) and 230° (LD_{1a}). Interference between the two axial directions produced dome and basin structures with radii in the range of 5–6 km. The Giaccuru dome (Figure 2) is especially distinctive, as its core hosts extensive mineralized skarns. The LD_1a 230°-plunging folds clearly preceded the D_2 extensional structures (folds and low-angle shear zones), and are therefore interpreted to have been related to shortening that occurred after nappe emplacement. As the relative timing of LD_1 and LD_1a is difficult to determine, their contemporaneous formation as the result of uniaxial symmetrical shortening cannot be ruled out.

5.3. Extensional post-collisional phase (Riu Gruppa phase)

In the study area, particularly around late-collisional dome structures (Serra Fenabrus, Giaccuru, close to M. Carraxiu, Cuccuru San Gabriele, Bruncu su Morgueu), the extensional phase generated low-angle ductile shear zones that enhanced the antiformal shape acquired during the late-collisional stage. In some areas, these shear zones reactivated previously developed thrusts into normal-sense shear zones. This

dynamic deformation resulted in a wide variety of tectonic transport directions related to the extensional phase. In the north flank of the Giaccuru antiformal dome, just south of Monte s'Iscova, kinematic indicators in gently dipping ductile shear zones demonstrate top-to-the-north motion, which contrasts with the overall direction of nappe emplacement during the collisional phase.

D_2 asymmetric folds, produced by vertical shortening at the expense of steeply dipping foliations are widespread on the flanks of antiformal domes, where they were developed at meter-scale with characteristic centrifugal vergence respect to the antiformal crests. The trends of D_2 fold axes are highly variable (see stereographic projection of Variscan structural elements included in the Main Map).

6. Ore deposit geology

Several types of ore deposits characterize the Gadoni district, and the most important of which are in the Giaccuru and Funtana Raminosa areas (Figure 5; Dessau, 1937; Minzoni, 1988; Ogniben & Monese, 1973; Revello & Chiorboli, 1970).

The lode deposit of Giaccuru is the largest Fe-skarn in Sardinia, with some mining explorations ascertaining more than 8×10^6 t of magnetite. Locally, Zn dominates over Fe in the form of sphalerite, and traces of galena are also present (Stara, Rizzo, Sabelli, & Ibba, 1999). The skarn mainly formed through the interaction between supercritical fluids and the Silurian–Devonian carbonate–shale succession; less commonly they developed at the expense of meta-basite (and this is quite common within a thermal aureole) or – in a couple of cases – within the meta-greywackes of the ORR Formation. The mineral assemblage includes garnet that dominantly has an andradite–grossularite composition, with very low contents of spessartine and pyrope (1–2%). Andradite prevails in proximity to Zn-skarns, whereas grossular is ubiquitous and invariably associated with magnetite. Pyrope-rich garnet occurs locally. Amphibole is invariably actinolite. Pyroxene is hedenbergite–diopside with minor amounts of johannsenite. Epidote is generally localized in veins that cross-cut massive magnetite and is associated with pyrite. Zoisite is common even though allanite is not rare. The epidote group minerals are interpreted as retrograde, and were probably associated with late circulation of epithermal fluids. It is estimated that andradite and pyrope-rich garnet formed at temperatures upward of 500°C, whereas epidote and pyrite–pyrrhotite associations formed at temperature below 300°C. The skarn of the Giaccuru lode deposit is localized in the core of the domal antiform that possibly acted as structural trap for fluids, similarly with other areas in the Variscan basement of SE Sardinia (Funedda et al., 2011).

In the Funtana Raminosa deposit (Figure 5), the ore is mainly composed of mixed Zn–Pb–Cu–Fe sulfides with minor bismutinite and magnetite. Silver occurs in approximately 500 ppm abundance and is rarely in its native form or in the form of its own mineral phases. Apart from these minerals of economic interest, numerous other primary sulfides were documented in mine reports, including the Cd phase hawleyite. The samples we analyzed were collected from mine tailings and from some outcrops in the San Gabriele area. Amongst the gangue silicates, the occurrence of ilvaite in addition to grossular–andradite garnet and diopside suggests temperatures greater than 500°C. High-temperature sulfides (>450°C) are represented by remnants of a solid solution between chalcopyrite and sphalerite (Sugaki, Kitakaze, & Kojima, 1987) within sphalerite crystals. Retrograde mineral associations include occurrences of epidote and galena that crystallized in fractures. Geological mapping showed that the Funtana Raminosa deposits are linked to granodiorite, which crops out a few hundred meters from the main mineralized area. Where metasomatism has affected carbonate boudins, the mineralization is mainly disseminated to massive. Regardless, metasomatism is enhanced by deformation cleavage and micro-shear zones that acted as preferential pathways for metal-rich fluids.

In the Funtana Raminosa area, apart from the skarn ores, the radiometric survey revealed elevated REE concentrations in Late Ordovician transgressive meta-sedimentary strata. This concentration is attributed to a placer-type accumulation of heavy minerals, such as ilmenite, zircon, and monazite. In thin section, heavy minerals are aligned in dark, transposed, mm-sized layers within the ORR Formation. Analyses using inductively coupled plasma mass spectrometry and instrumental neutron activation analysis methods revealed $\sum$REE values of 4000–6000 ppm. Such high values suggest that the area may be of economic interest and worthy of additional investigation.

7. Conclusions

The geological map of the Gadoni area presents detailed geological mapping of Variscan basement exposed in central Sardinia. In this area, only a few localized, outdated maps (1:100,000 scale Geological Survey of Italy; Bosellini & Ogniben, 1968) were previously available, which loosely distinguished different terrigenous deposits and did not consider the polyphase Variscan tectonic history. The gamma-ray survey allowed us to overcome the challenge of differentiating meta-sedimentary strata that belonged to distinct tectonic units, resulting in a more accurate geological map of the tectonic units and related formations. Fieldwork and structural analysis reveal that the Giaccuru dome is a late-collisional structural high built by the interference between 130°-trending and newly discovered 050°-

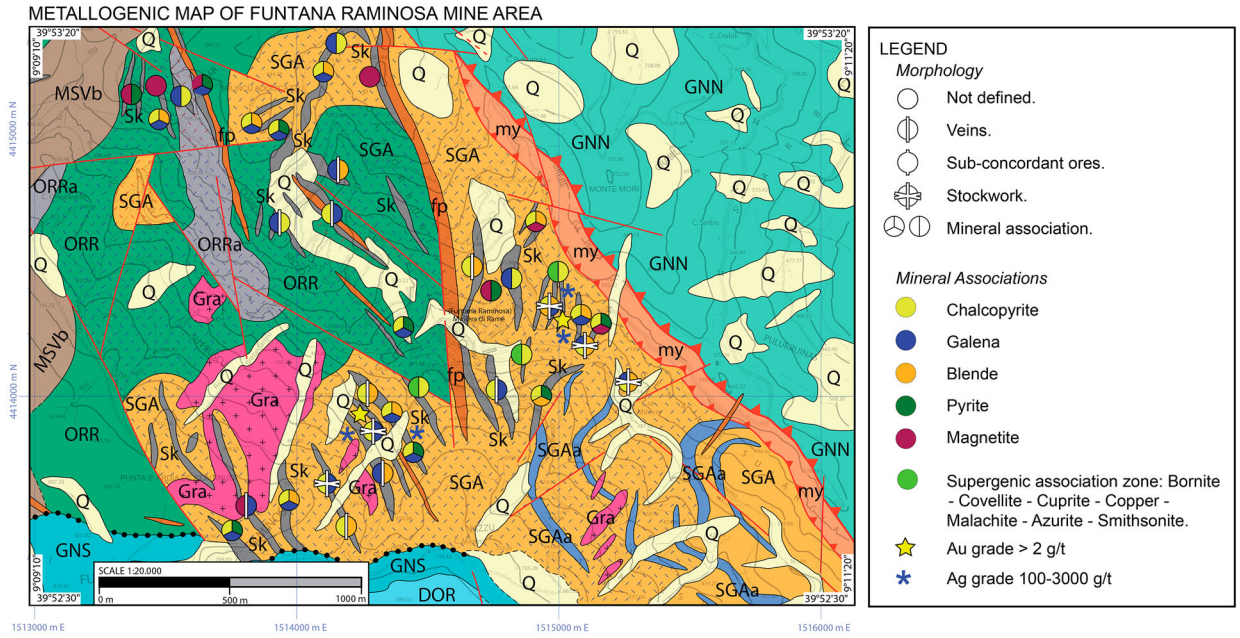

Figure 5. Ore deposit sketch map of the Gadoni area.

trending antiforms. The post-collisional extension was sub-contemporaneous with the 299 ± 3 Ma emplacement of Gra, and enhanced the dome structure.

The mapped structural relationships suggest that important skarns of the Gadoni district formed in relation to the emplacement of the Granodiorite. Additionally, the skarns were mainly controlled by occurrences of Silurian–Devonian carbonate slices dispersed as several boudins and in fold hinges during the main Variscan deformation event. Late Ordovician transgressive meta-sedimentary rocks show interesting elevated REE concentrations (4000–6000 ppm) that are worthy of further exploration.

Software

The map was compiled by digitally tracing geological contacts from a scanned version of a hand-drawn map using Adobe Illustrator CS6.

Acknowledgements

We are grateful to Alfredo Loi for the availability of his portable gamma-ray spectrometer and to Salvatore Marceddu for his help with electron dispersive spectroscopy microanalyses. D. J. Weary and G. Musumeci are thanked for their careful reviews.

Disclosure statement

No potential conflict of interest was reported by the authors.

Funding

This work was supported by the University of Sassari Ph.D. fund granted to M. M. and by LR/7 RAS funds granted to G. O. The work of A. F. was partially supported by the Fondazione di Sardegna fund (PRID; University of Cagliari).

ORCID

Giacomo Oggiano http://orcid.org/0000-0003-1236-1498

References

Amadesi, E., Cantelli, C., Carloni, G. C., & Rabbi, E. (Cartographer). (1967). Carta geologica del Foglio 208-Dorgali.

Bosellini, A., & Ogniben, G. (1968). Ricoprimenti ercinici nella Sardegna centrale. *Annali dell'Università di Ferrara*, *1*, 1–15.

Calvino, F. (1959). Lineamenti strutturali del Sarrabus-Gerrei (Sardegna sud-orientale). *Bollettino del Servizio Geologico d'Italia*, *81*(4–5), 489–556.

Calvino, F., Dieni, I., Ferasin, F., & Piccoli, G. (Cartographer). (1972). Note illustrative della Carta Geologica d'Italia, in scala 1:100.000, Foglio 195-Orosei.

Carmignani, L., Cocozza, T., Ghezzo, C., Pertusati, P. C., & Ricci, C. A. (1982). Lineamenti del basamento sardo. In L. Carmignani, T. Cocozza, C. Ghezzo, P. C. Pertusati, & C. A. Ricci (Eds.), *Guida alla Geologia del Paleozoico Sardo* (pp. 11–23). Cagliari: Società Geologica Italiana. Guide Geologiche Regionali.

Carmignani, L., Conti, P., Barca, S., Cerbai, N., Eltrudis, A., Funedda, A. (2001). *Foglio 549-Muravera. Note illustrative*. Roma: Servizio Geologico d'Italia.

Carmignani, L., Oggiano, G., Funedda, A., Conti, P., & Pasci, S. (2015). The geological map of Sardinia (Italy) at 1:250,000 scale. *Journal of Maps*. doi:10.1080/17445647.2015.1084544

Carosi, R., & Pertusati, P. C. (1990). Evoluzione strutturale delle unità tettoniche erciniche nella Sardegna centro-meridionale. *Bollettino della Società Geologica Italiana*, *109*, 325–335.

Casini, L., Cuccuru, S., Maino, M., & Oggiano, G. (2015). Structural map of Variscan northern Sardinia (Italy). *Journal of Maps*, *11*(1), 75–84.

Casini, L., & Oggiano, G. (2008). Late orogenic collapse and thermal doming in the northern Gondwana margin

incorporated in the Variscan Chain: A case study from the Ozieri Metamorphic Complex, northern Sardinia, Italy. *Gondwana Research*, *13*, 396–406.
Cassinis, G., Durand, M., & Ronchi, A. (2003). Permian-Triassic continental sequences of Northwestern Sardinia and South Provence: Stratigraphic correlations and palaeogeographical implications. *Bollettino della Società Geologica Italiana*, *2*, 119–129.
Conti, P., Carmignani, L., & Funedda, A. (2001). Change of nappe transport direction during the Variscan collisional evolution of central-southern Sardinia (Italy). *Tectonophysics*, *332*(1–2), 255–273.
Conti, P., Carmignani, L., Oggiano, G., Funedda, A., & Eltrudis, A. (1999). From thickening to extension in the Variscan belt – kinematic evidence from Sardinia (Italy). *Terra Nova*, *11*(2–3), 93–99. doi:10.1046/j.1365-3121.1999.00231.x
Conti, P., & Patta, E. D. (1998). Large scale W-directed tectonics in southeastern Sardinia. *Geodinamica Acta*, *11*(5), 217–231.
Corradini, C., & Ferretti, A. (2009). The Silurian of the external Nappes (southeastern Sardinia). *Rendiconti della Società Paleontologica Italiana*, *48*(1), 43–49.
Corradini, C., Ferretti, A., & Serpagli, E. (1998). The Silurian and Devonian sequence in SE Sardinia. *Giornale di geologia*, *60*(ECOS VII - special issue), 71–74.
Costamagna, L., Barca, S., & Lecca, L. (2007). The Bajocian-Kimmeridgian Jurassic sedimentary cycle of Eastern Sardinia: stratigraphic, depositional and sequence interpretation of the new 'Baunei group'. *Comptes Rendus Geoscience*, *339*(9), 601–612.
Cuccuru, S., Naitza, S., Secchi, F. A., Puccini, A., Casini, L., & Pavanetto, P. (in press). Structural and metallogenic map of late Variscan Arbus Pluton (SW Sardinia, Italy). *Journal of Maps*, 1–6. doi:10.1080/17445647.2015.1091750
Del Rio, M. (1985). Palynology of Middle Jurassic black organic shales of 'Tacco di Laconi', Central Sardinia, Italy. *Bollettino della Società Paleontologica Italiana*, *23*(2), 325–342.
Demant, A., & Coulon, C. (1973). Sur la présence de laves à affinités calco-alcalines au sein du volcanisme alcalin plio-quaternaire de la Sardaigne nord-occidentale. *Comptes Rendus de l'Académie des Sciences de Paris*, *D*(276), 3073–3076.
Dessau, G. (1937). Studi sulla miniera di Fontana Raminosa (Sardegna). *Periodico di Mineralogia*, *2*, 177–215.
Dessau, G., Duchi, G., Moretti, A., & Oggiano, G. (1982). Geologia della zona del Valico di Correboi (Sardegna centro-orientale). Rilevamento, tettonica e giacimenti minerari. *Bollettino della Società Geologica Italiana*, *101*, 497–522.
Dieni, I., Fischer, J. C., Massari, F., Salard-Cheboldaeff, M., & Vozenin-Serra, C. (1983). La succession de Genna Selole (Baunei) dans le cadre de la paléogéographie mésojurassique de la Sardaigne orientale. *Memorie della Società Geologica Italiana*, *36*, 117–148.
Dieni, I., & Massari, F. (1985). Mesozoic of Eastern Sardinia. In A. Cherchi (Ed.), *19th European Micropaleontological Colloquium* (pp. 66–78). Cagliari: Agip.
Dieni, I., & Massari, F. (1987). Le Mésozoique de la Sardaigne orientale. In A. Cherchi (Ed.), *Groupe Française du Crétacé* (pp. 125–134). Cagliari: Excursion en Sardaigne.
Di Milia, A. (1991). Upper Cambrian Acritarchs from the Solanas sandstone Formation, Central sardinia, Italy. *Bollettino della Società Paleontologica Italiana*, *30*(2), 127–152.
Funedda, A., Meloni, M. A., & Loi, A. (2015). Geology of the Variscan basement of the Laconi-Asuni area (central Sardinia, Italy): The core of a regional antiform refolding a tectonic nappe stack. *Journal of Maps*, *11*(1), 146–156. doi:10.1080/17445647.2014.942396
Funedda, A., Naitza, S., Conti, P., Dini, A., Buttau, C., & Tocco, S. (2011). The geological and metallogenic map of the Baccu Locci mine area (Sardinia, Italy). *Journal of Maps*, *7*(1), 103–114. doi:10.4113/jom.2011.1134
Gaggero, L., Oggiano, G., Funedda, A., & Buzzi, L. (2012). Rifting and arc-related early Paleozoic volcanism along the North Gondwana margin: geochemical and geological evidence from Sardinia (Italy). *Journal of Geology*, *120*(3), 273–292. doi:10.1086/664776
Gattiglio, M., & Oggiano, G. (1990). L'unità tettonica di Bruncu Nieddu e i suoi rapporti con le unità della Sardegna sud-orientale. *Bollettino della Società Geologica Italiana*, *109*, 547–555.
Hawkesworth, C. J., Turner, S. P., McDermott, F., Peate, D. W., & Van Calsteren, P. (1997). U-Th isotopes in arc magmas: Implications for element transfer from the subducted crust. *Science*, *276*(5312), 551–555.
Loi, A., Barca, S., Chauvel, J. J., Dabard, M. P., & Leone, F. (1992). Analyse de la sédimentation post-phase sarde: les dépôts initiaux à placers du SE de la Sardaigne. *Comptes Rendus de la Société Géologique de France, serie II*, *315*(2), 1357–1364.
Minzoni, N. (1975). La serie delle formazioni paleozoiche a Sud del Gennargentu. *Bollettino della Società Geologica Italiana*, *94*, 347–365.
Minzoni, N. (1988). Geologia strutturale della zona di Gadoni-Funtana Raminosa (Sardegna centrale). *Memorie di Scienze Geologiche*, *40*, 195–201.
Naud, G. (1979). Les shales de Rio Canoni, formation-repère fossilifère dans l'Ordovicien supérieur de Sardaigne orientale. Conséquences stratigraphiques et structurales. *Bulletin de la Société géologique de France*, *21*(2), 155–159.
Oggiano, G. (1994). Lineamenti stratigrafico-strutturali del basamento del Goceano (Sardegna centro-settentrionale). *Bollettino della Società Geologica Italiana*, *113*, 105–115.
Oggiano, G., Gaggero, L., Funedda, A., Buzzi, L., & Tiepolo, M. (2010). Multiple early Paleozoic volcanic events at the northern Gondwana margin: U-Pb age evidence from the Southern Variscan branch (Sardinia, Italy). *Gondwana research*, *17*(1), 44–58. doi:10.1016/j.gr.2009.06.001
Ogniben, G., & Monese, A. (1973). Il 'Gran Dicco' (Giacimento di Funtana Raminosa-Sardegna). *Memorie degli Istituti di Geologia e Mineralogia dell'Universita di Padova*, *29*, 1–36.
Pertusati, P. C., Sarria, E., Cherchi, G. P., Carmignani, L., Barca, S., & Benedetti, M. (2002). Note illustrative del F° 541-Jerzu. *Note illustrative della Carta geologica d'Italia alla scala 1:50.000*, 169.
Plank, T., & Langmuir, C. H. (1998). The chemical composition of subducting sediment and its consequences for the crust and mantle. *Chemical Geology*, *145*(3), 325–394.
Revello, G., & Chiorboli, S. (1970). Sulla presenza di associazioni di cubanite, calcopirite, pirrotina, blenda e mackinawite incluse in quarzo a Funtana Raminosa (Sardegna). *Periodico di Mineralogia*, *39*, 211–217.
Šimíček, D., Bàbek, O., & Leichmann, J. (2012). Outcrop gamma-ray logging of siliciclastic turbidites: Separating the detrital provenance signal from facies in the foreland-basin turbidites of the Moravo-Silesian basin,

Czech Republic. *Sedimentary Geology*, *261–262*, 50–64. doi:10.1016/j.sedgeo.2012.03.003

Stara, P., Rizzo, R., Sabelli, C., & Ibba, A. (1999). I minerali di Funtana Raminosa (Gadoni, Sardegna centrale). *Rivista Mineralogica Italiana*, *1*, 10–27.

Sugaki, A., Kitakaze, A., & Kojima, S. (1987). Bulk compositions of intimate intergrowths of chalcopyrite and sphalerite and their genetic implications. *Mineralium deposita*, *22*, 26–32.

Tongiorgi, M., Albani, R., & Di Mila, A. (1984). The Solanas sandstones of Central Sardinia: New paleontological data (Acritarchs) and an attempt of geological interpretation (a 'post-sardinian' molasse?). *Bulletin de la Société Géologique de France*, *26*(4), 665–680.

Vai, G. B., & Cocozza, T. (1974). Il 'Postgotlandiano' sardo, unità sinorogenica ercinica. *Bollettino della Società Geologica Italiana*, *93*, 61–72.